Nigerian Journal of Physics (NJP)
ISSN online: 3027-0936
ISSN print: 1595-0611
DOI: https://doi.org/10.62292/njp.v33i2.2024.212
Volume 33(2), Special Issue, June 2024

Integrated Geophysical Investigation for Potential Gold Mineralised Zone within Lower Part of Zuru Schist Belts, NW Nigeria

***[1]Augie, A. I., [2]Salako, K. A., [2]Rafiu, A. A. and [3]Jimoh, M. O.**

[1]Applied Geophysics Department, Federal University Birnin Kebbi, Nigeria
[2]Geophysics Department, Federal University of Technology Minna, Nigeria
[3]Geology Department, Federal University of Technology Minna, Nigeria.

[*]Corresponding author's email: ai.augie@fubk.edu.ng Phone: +2348137330559

ABSTRACT

The study began with a reconnaissance survey that used high-resolution aeromagnetic data of the study area to identify suitable structure zones with the potential to trap mineral resources within the context of the gold exploration target. The findings of magnetic studies were followed up with detailed investigations using 2D electrical resistivity tomography (ERT) and induced polorisation (IP) techniques to reveal further details about gold mineral zones and other lithological boundaries. The airborne magnetic data of sheet 118_Yelwa was obtained from the NGSA; these datasets were processed and analyzed using Oasis Montaj's first vertical derivative (FVD) and center for exploration targeting (CET) techniques. Results of FVD and CET grid anomalies show that regions of major magnetic structures (lineaments) are associated with granite gneiss, migmatitic augen gneiss, and medium to coarse-grained biotite when compared to the geological settings of the area. The zones of major structures obtained in this study coincided with previous magnetic studies of the area, located in the eastern parts of Ngaski, Yauri (Yelwa), Shanga, Agwara, as well as Magama's northwest region. Some of the regions for lineament (in the eastern part of Ngaski/Yauri) were investigated further with 2D ERT and IP detailed geophysical methods in a dipole-dipole configuration. The results of geoelectric techniques along profiles 1, 2, and 3 identified the major gold mineralisation potential zones, which were labeled **A1**, **A2**, and **A3**. These regions have low/high resistivity (1.6 to 459 Ωm/1889 to 7773 Ωm) and chargeability signatures (≥ 20 msec), and could thus be interpreted as potential target zones for metallic mineral exploration, particularly gold mineralisation. The regions are located in the northern Mararraba and southwest of the Jinsani areas of Kebbi State. The results of integrated geophysical methods have produced updated structural features of the regions, as well as a database containing precise locations, lateral lengths, thicknesses, and depths for prospective gold mineralisation zones. This database could assist the miner/explorer in locating the potential zone of gold mineralisation.

Keywords:
Gold Mineralisation Zones, Mineral Exploration, Zuru Schist Belt, Aeromagnetic, Electrical Resistivity Tomography (ERT), Induce Polarisation (IP).

INTRODUCTION

In Nigeria, the majority of gold deposits are found in quartz veins, but there are also gold inclusions in specific ore minerals in a range of metasedimentary and meta-igneous rocks found throughout the different supracrustal schist belt strata (Ramadan and Abduel-Fattah, 2010; Aliyu *et al.*, 2021). Numerous artisanal projects have been undertaken in Nigeria's gold fields, focusing on major gold-quartz reefs and the alluvial deposits (Garba, 2000; Sani *et al.*, 2019; Adetona *et al.*, 2019). To create a database with exact coordinates and locate the zones that contain these gold minerals, geophysical studies are necessary (Augie *et al.*, 2022a). Numerous qualitative and quantitative geophysical studies were carried out in the research area to try and pinpoint potential zones for mineralisation. Aeromagnetic data over the current study area was analyzed by Bonde *et al.* (2019), Lawali *et al.* (2020), Augie *et al.* (2021, 2022a&b) in order to identify structural potential mineralisation zones. The enhancing filters employed in the study include tilt derivatives (TDR), first vertical derivatives (FVD), second vertical

derivatives (SVD), and analytical signal (AS). The study's findings led to the identification of NE-SW-oriented structures, such as veins and fractures, where economic minerals are typically hosted. However, because the study solely relied on aeromagnetic data obtained from secondary sources, the findings from those literatures requires ground trothing (to confirm what the magnetic suveys found). Comprehensive investigations using 2D electrical resistivity imaging (ERI) and induced polarisation (IP) geophysical techniques were not conducted in order to further investigate the anomalous zones identified by aeromagnetic study.

Aisabokhae (2021) and Lawal *et al.* (2021) investigated potential mineralisation zones in the Kebbi south using aeromagnetic and aero-radiometric datasets. Reduction to the magnetic equator (RTE), AS, FVD, Euler deconvolution (ED), composite image, ratio maps, and ternary image were the enhancement filtering techniques used in the study. According to the study's conclusions, the Anka schist region is situated on the periphery of a plutonic area that displays brittle-ductile distortion, indicating structural fracture for fluid flow and related alteration brought on by hydrothermal events toward mineralisation in the areas. There are, however, gaps in the literature because the study area is within equatorial zones of low latitude, and the authors did not centralize the anomalies effectively using the magnetic equator. Holden *et al.* (2008), Core *et al.* (2009) state that at these regions, an additional amplitude correction is usually necessary to keep the north-south signal in the data from dominating the results. Using in-depth techniques like 2D ERT and IP geophysical methods for the identification of mineralised potential zones, the anomalous zones found in the study were not investigated further.

However, to identify the structures that might support gold mineralisation throughout Kebbi South, Augie *et al.* (2021, 2022a&b) analyzed the magnetic signatures in conjunction with the local geological context. The research employed the subsequent methodologies: RTE, FVD, SVD, CET, TDR, ED, SPI, and 2D magnetic modeling. The delineation of lineaments such as faults and fractures, particularly shear zones believed to be associated with alteration zones, was made easier by the results of these techniques and is an important aspect of defining gold mineralised prospects according their findings. In comparison related geological setting, the structures identified within it are associated with granite, gneiss, quartz-mica schist, diorite, biotite hornblende granite, and medium coarse-grained granite. These techniques' outcomes revealed alteration zones that might contain gold. The SE parts of Yelwa (Yauri), Shanga, Magama, Fakai, Rijau, Zuru, Ngaski, and the eastern sections of Bukkuyum and Wasagu/Danko are the locations of these potential zones.

This study used integrated geophysical methods, including aeromagnetic, 2D ERT, and IP techniques, to identify subsurface structures, resistivity, and chargeability signature zones in the study area. The structural features could be important in the exploration of mineral resources, particularly gold minerals. The research began with a reconnaissance survey that used high-resolution aeromagnetic data of the study area to identify suitable structure zones that have the potential to trap mineral resources in the context of the gold exploration target. As a follow-up geophysical technique, the 2D ERT and IP revealed more details on gold mineral zones and other lithological boundaries.

The study Area

The study area lies between latitudes 10°30′0″N and 11°0′0″N and longitudes 4°30′0″E and 5°0′0″E in Kebbi South and some parts of Niger State. The following local government areas (LGAs) are included in the area: Agwara, Ngaski, Shanga, Magama, and the SE portion of Yauri (Figure 1). In terms of geology, the region is located in northwest Nigeria's basement complex regions. Mangrove swamps, the Pan-African Older Granitoid, the Gwandu Formation, and Nupe Sandstone all underlie the region (Olugbenga and Augie, 2020). According to Figure 1, these included Phyllite, Medium to Coarse-Grained Biotite, Migmatitic Augen Gneiss, Granite Gneiss, Sands, Clays, Fieldspathic, Sandstones, Siltstones, Mangrove Swamps, and Undifferentiated Schists.

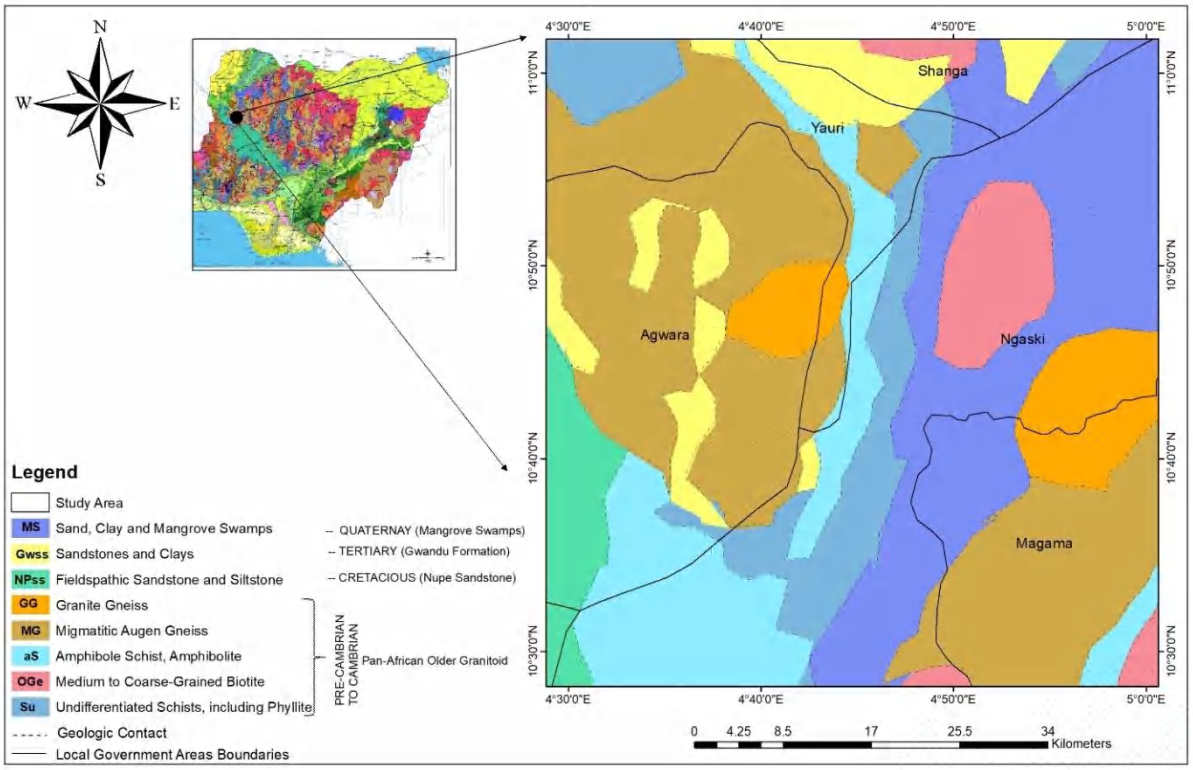

Figure 1: Location and geological setting of the study area (modified after NGSA, 2007)

MATERIALS AND METHODS

Methods

Airborne Magnetic Method

The present study used the aeromagnetic data sheet 117_Yelwa, which covered the study region. The data were obtained from the Nigerian Geological Survey Agency (NGSA). These datasets were gathered between 2005 and 2009 by Fugro Airborne Survey on behalf of the Nigerian government's NGSA. The data were collected at a terrain clearance of 100 meters, with flight lines spaced 500 meters and tie lines spaced 2000 meters, all of which were oriented NW-SE. The maps have a 1:100,000 scale and are half-degree sheeted.

The main/core field was used to remove the geomagnetic gradient (International Geomagnetic Reference Field, IGRF) in order to correct the acquired data. The magnetic anomaly (TMI anomaly) was calculated by subtracting the generated core fields (DGRF for the epoch period) from the grid values (TMI). The magnetised body anomaly, which is usually dependent on the orientation of the body with respect to magnetic north, inclination, declination, and local earth's field, has been highlighted by reducing the TMI anomaly map to the magnetic equator. These data were further processed, enhanced, and interpreted using first vertical derivative (FVD), analytic signal (AS), and center for exploration targeting (CET) techniques using Geosoft (Oasis Montaj), Arc GIS, and Surfer software.

In order to improve closely spaced resolution and superimposed anomalies, the FVD technique helps to attenuate long-wavelength magnetic anomalies within the field. Major geological structures may be located in these anomalous zones. The linear structures (lineament) that are revealed by CET can define faults, fractures, or shear zones that correspond to mineralisation veins.

2D Geoelectric Prospecting Method

In this study, a 2D geoelectrical survey was also conducted at the Yauri/Ngaski boundaries of Kebbi state in northwest Nigeria. A dipole-dipole configuration with a minimum electrode spacing (a) of 10.00 meters was used to investigate fields covering an area of 640 m^2. Three profiles were carried out for each 300-meter distance along the profile, oriented NW-SE (Figure 2).

The data were collected with a Super Sting (resistivity meter) connected to an electrode selector and powered by a 12 V battery. This instrument is capable of measuring both apparent resistivity and IP data simultaneously. The distance between the two pairs of current electrodes (C1 and C2) was determined to be the same as the distance between the two potential electrodes. The distance between C1 and P1 (dipole separation factor) was calculated as a multiple of an integer n of the distance between C1-C2 and P1-P2 (Figure 3).

The dipole separation factor n was first set to one (1), then increased to two (2), three (3), and so on until it reached a maximum of eight (8). Thus, the two parameters, dipole separation factor (n) and space between the current electrode pair (a), have been measured. The measurements were taken with electrode separation of 10 m and n set to 1, 2, 3, … 8 (Figure 3). As the n increases, so does the electrode spacing, and the injected current flows to greater depths (Loke and Barker, 1996; Loke, 2000; Wahyu, 2016).

The initial measurement was performed using electrodes 1, 2, 3, and 4 (C1, C2, P1, and P2). C2 was used at 0 meters, C1 at 10 meters, P1 at 20 meters, and C2 at 30 meters. Similarly, in the second measurement, C2 was at 10 m, C1 at 20 m, P1 at 30 m, and P2 at 40 m. The above steps were repeated along the profile line at 1*a*, 2*a*, 3*a*, 4*a*, 5*a*, 6*a*, 7*a*, and 8*a* intervals between C1 and P1, where *a* is 10 m. At each measurement, the ground apparent resistivity and IP values were measured. The obtained data were analyzed using Loke's (1999) RES2DINV program, which automatically generates 2D resistivity and IP models for the subsurface.

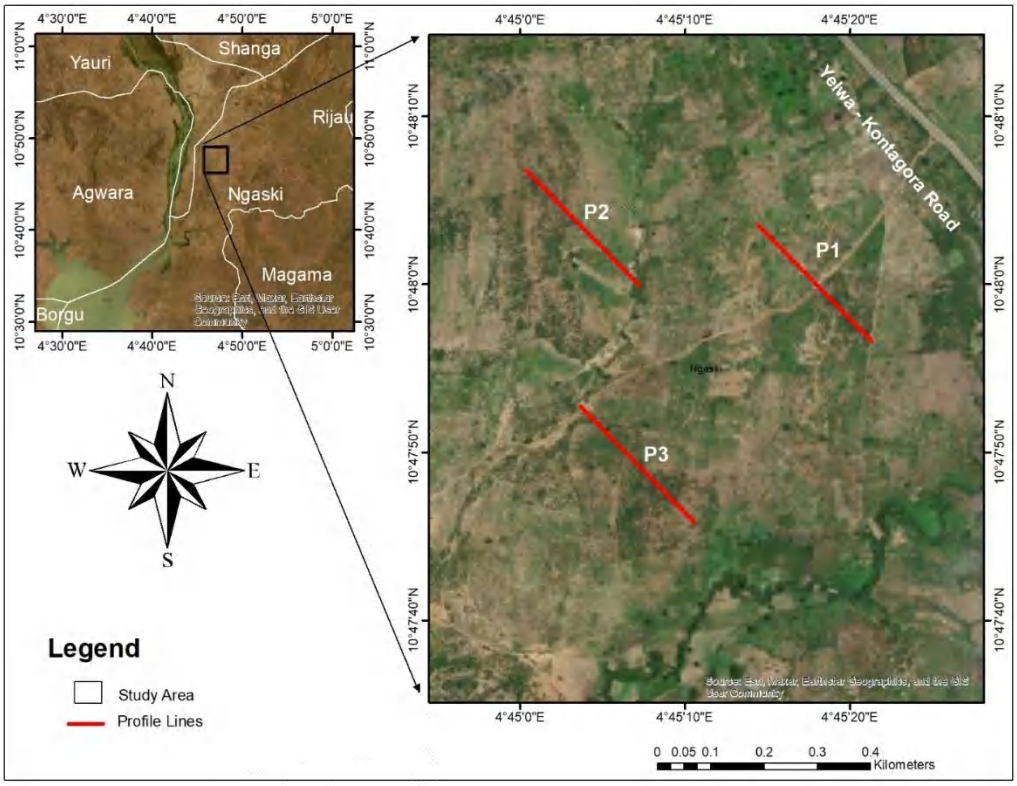

Figure 2: Profile line field survey layout

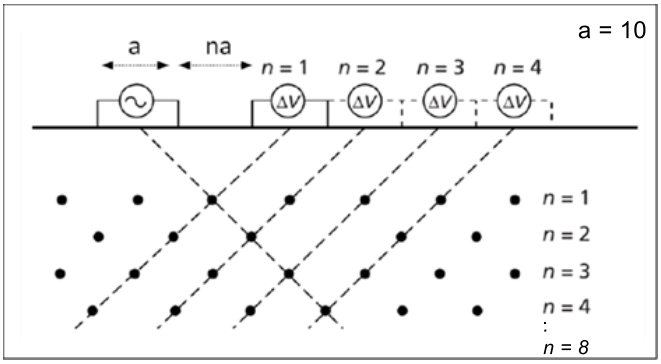

Figure 3: Illustration of dipole-dipole array for the field procedure of this research

RESULTS AND DISCUSSION

Airborne Magnetic Method Results

This study started off with a reconnaissance survey using the aeromagnetic method. The processing techniques employed were total magnetic intensity reduced to the magnetic equator (TMI-RTE), first vertical derivative (FVD) and center for exploration (CET).

TMI Result

Figure 4 depicts the colour image of IGRF, which representets the corrected total magnetic intensity (TMI). The map represents the vector sum of all magnetic field components. Its primary purpose in this study is to reveal the magnetic properties of the various lithological units in the area. The magnetic signatures vary in intensity from low to high. The low magnetic regions have a magnetic susceptibility of 32,917.06 nT (minimum) along the northeast region of the study area, which is located in northern Ngaski, eastern Yauri, and Shanga. High magnetic susceptibility zones of 33,119.0 nT (maximum) exist under the southeastern parts of the area, which are located in the southern part of Agwara, the northern part of Borgu, the eastern part of Ngaski, and the northern part of Magama.

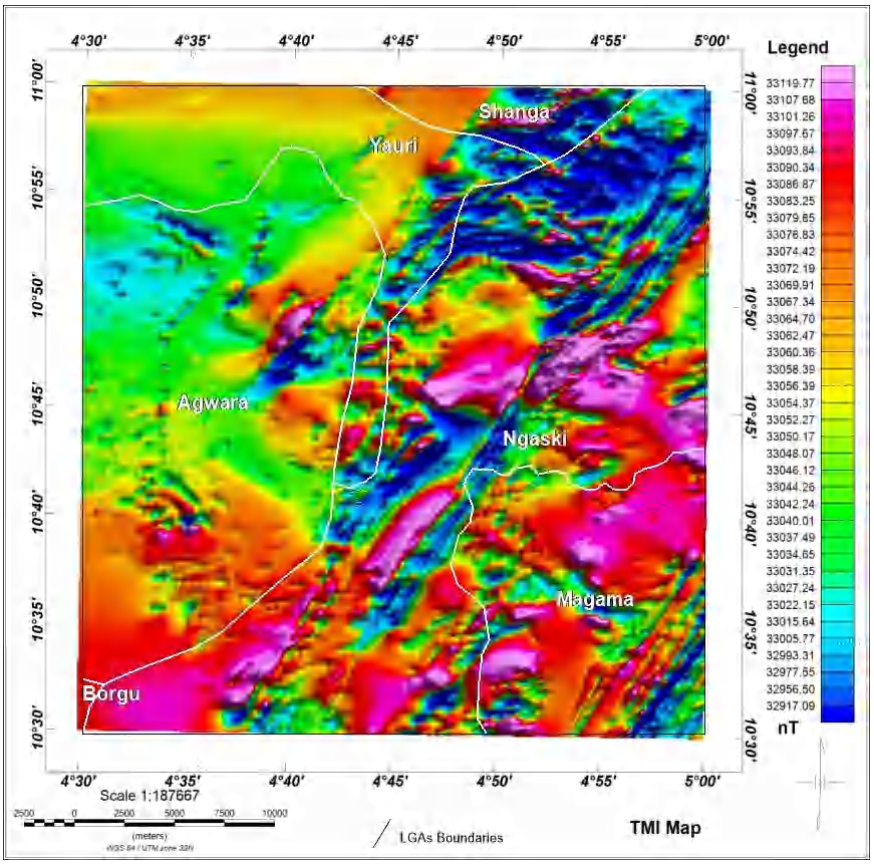

Figure 4: TMI map of the study area

RTE Result

TMI-RTE anomalies are represented by the composite color in Figure 5. High magnetic trend anomalies are indicated by the red or pink anomalies, with values ranging from -636.32 nT to -564.48 nT, which situated in the southwest regions of Shanga and Rijau, these areas are called Yauri. Areas with low magnetic anomalies are displayed in blue or green, and they lie between -734.68 nT and -656.79 nT. NE Shanga, Rijau, and Fakai are corresponding zones.

Thus, the magnetic susceptibility of rocks varies depending on the types of rock formations found in high and low regions (Figure 1). At lower depths than the Curie point isotherm, the susceptible rocks are typically found. The high negative values indicate high magnetic susceptibility zones. Figure 3 illustrates, the horizontal component of the Earth's magnetic field polarises all rocks in opposition to their magnetisation and the magnetic equator is a zone of zero inclination. When temporal effects such as the crustal field are subtracted from the measured field, the residual anomaly over magnetic materials is usually negative.

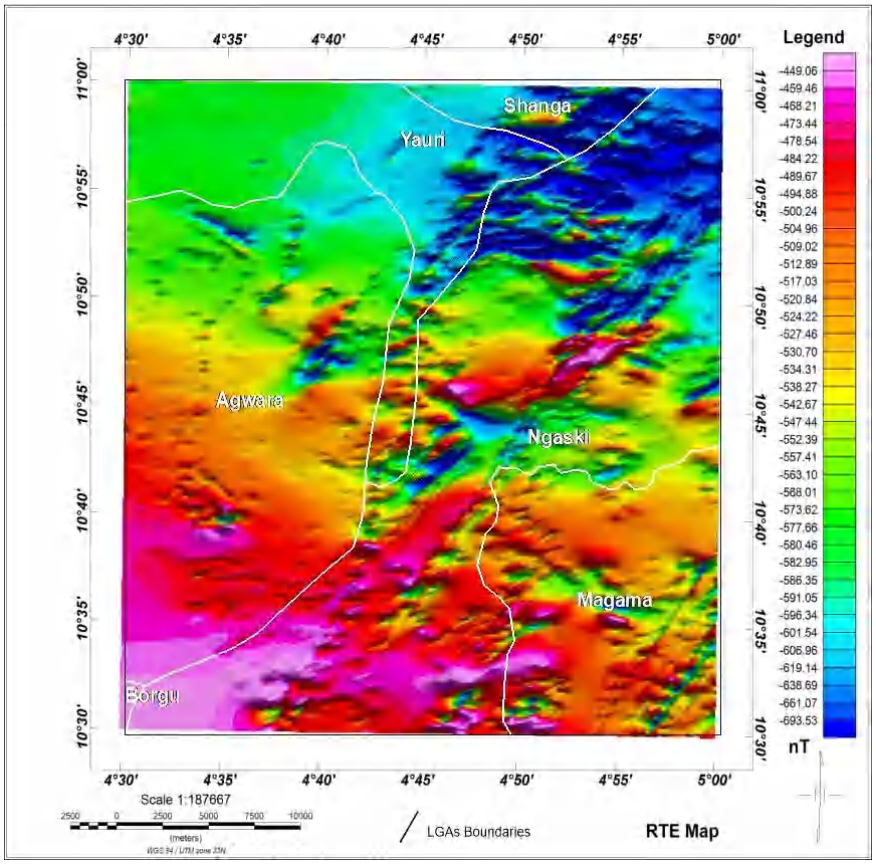

Figure 5: TMI-RTE map of the study area

FVD superimposed on CET lineaments Result

Figure 6 shows the FVD map, which attenuates long-wavelength magnetic anomalies within the field, improving closely spaced resolution and superimposed anomalies. The TMI-RTE map in Figure 3 did not previously display these anomalies. Figure 4 illustrates some regular linear structures that can be interpreted as lineaments that indicate fractures, faults, and joints. These lineaments were located in Shanga, Fakai, and Rijau's eastern region.

The resulting lineaments, as shown in Figure 6, are below the magnetic source's edge and may represent faults, fractures, or shear zones—all of which are frequently used as conduits for mineral deposits during hydrothermal processes. The combination of these structures controls the mineralization pattern, particularly in the lithium-bearing pegmatite of the study area. In contrast to the related geological setting, the areas are underlain by granite gneiss, migmatitic augen gneiss, medium to coarse-grained biotite, sands, clays, fieldspathic, and sandstones. These features and formations may act as potential mineral hosts.

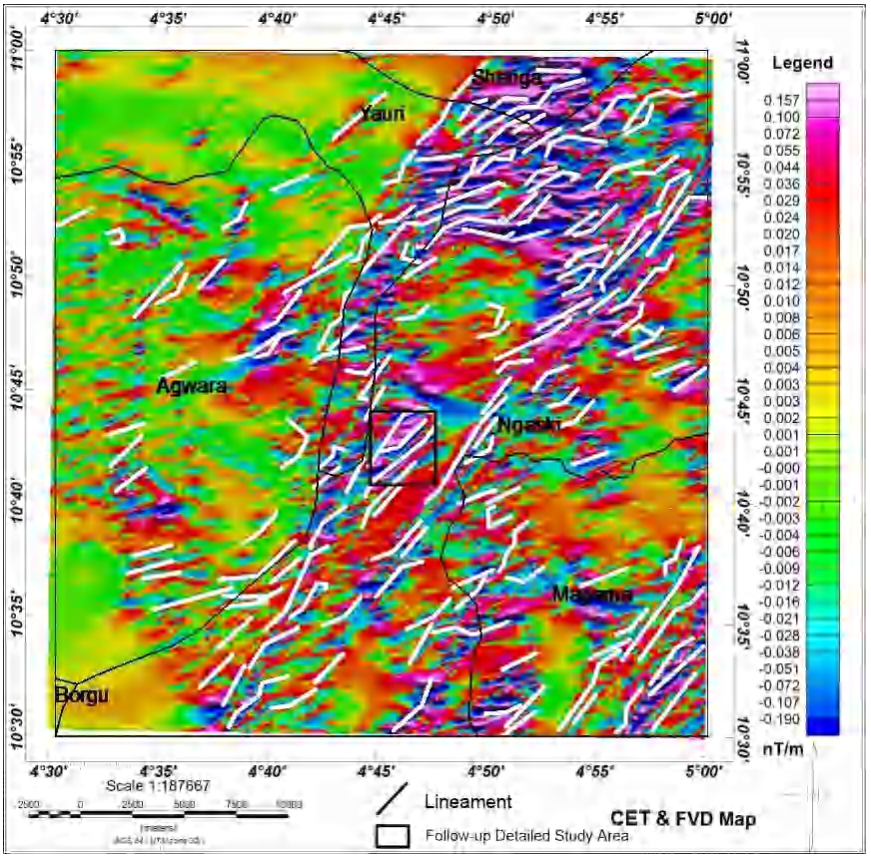

Figure 6: FVD map superimposed on CET lineaments map of the study

Results from 2D Geoelectric Prospecting Techniques

The area's geological setting influences how the 2D geoelectric modelled sections were interpreted in the research. These include resistivity values from earlier studies conducted in the same basement complex, which were utilised to correlate the findings of the current survey, and the borehole lithology of the southern part of Kebbi, obtained from RUWASA (Rural Water Supply and Sanitation Agency), as indicated in Table 1 (Osazuwa and Chii, 2010).

Table 1: A borehole/lithology log of the southern part of Kebbi areas (SARDA, 1988; Osazuwa and Chii, 2010)

Lithology	Depth(m)	Thickness(m)	Resistivity range (Ωm)
Lateritic Sand	0-2	2	60-1000
Highly Decomposed Schist	2-10	8	10-500
Partially Decomposed Granite	10-15	12	100-1000
Quartzite's and Gneiss	15-21	16	200-100000

Geoelectric Sections for Profile 1

The 2D inverse model section for profile 1 is shown in Figure 7(a). It has a lateral distance of 300 meters and it is oriented NW-SE. The profile is located between longitudes of 4°45'14.4"E to 4°45'21.6"E and latitudes of 10°48'3.6"N to 10°47'56.4"N (see Fig. 2). Four distinct zones were used to section the subsurface feature: **A1**, **Z1**, **A2**, and **Z2**. Zone **A1** is defined by resistivity values that range from 1.6 Ωm to 459 Ωm. These values are found on sections of the profile length that are 10-80 m, 190-200 m, and 250-265 m, respectively, and have a depth and thickness of 12.0 m, 18.5-24.9 m, and 7.5-18.5 m. Resistivity values in zone **A2** range from 1889 Ωm to 7773 Ωm. This range includes depth/thickness of 8-24.9 m, 3-24.9 m, 24.9 m, 24.8 m, and 7.5 m, as well as distances along the profile of 35-55 m, 70-92 m, 105-130 m, 145-180 m, 200-210 m, and 220-270 m.

Conversely, Zone **Z1** spans lengths of 30-110 m, 130-149 m, 190-200 m and 245-265 m, and corresponds to depths and thicknesses of 2.5-18.5 m, 24.9 m, 18.5 m and 2.5-18.5 m, in that order. Between 460 to 1888 Ωm

is its resistivity range. Zone **Z2**, on the other hand, has occupied a length of 100-125 m, 175-190 m, 200-250 m, and 265-290 m, with corresponding depth/thickness of 7.5-24.9 m, 12-24.9 m, 2.5-24.9 m, and 18.5 m, respectively. Its resistivity ranges from 7774 Ωm to 32002 Ωm.

When features **A1**, **Z1**, **A2**, and **Z2** are compared to Table 1, the subsurface lithology could consist of lateritic soil, highly decomposed schist, partially decomposed granite and quartzite, and quartzite/gneiss. On the other hand, zone **A1's** low resistivity regions might be a result of water persisting in the oxidized rock. This type of oxidized rock that comes from rhyolite or granite may host some minerals, especially gold. Granite and quartzite that have partially decomposed into dykes are associated with Zone **A2**. Finding the gold mineral may depend on the aforementioned rock formation's dyke subsurface structures. The inverse model section's results, which are displayed in Figure 7a, were further processed to create a geologic section, which is depicted in Figure 7b.

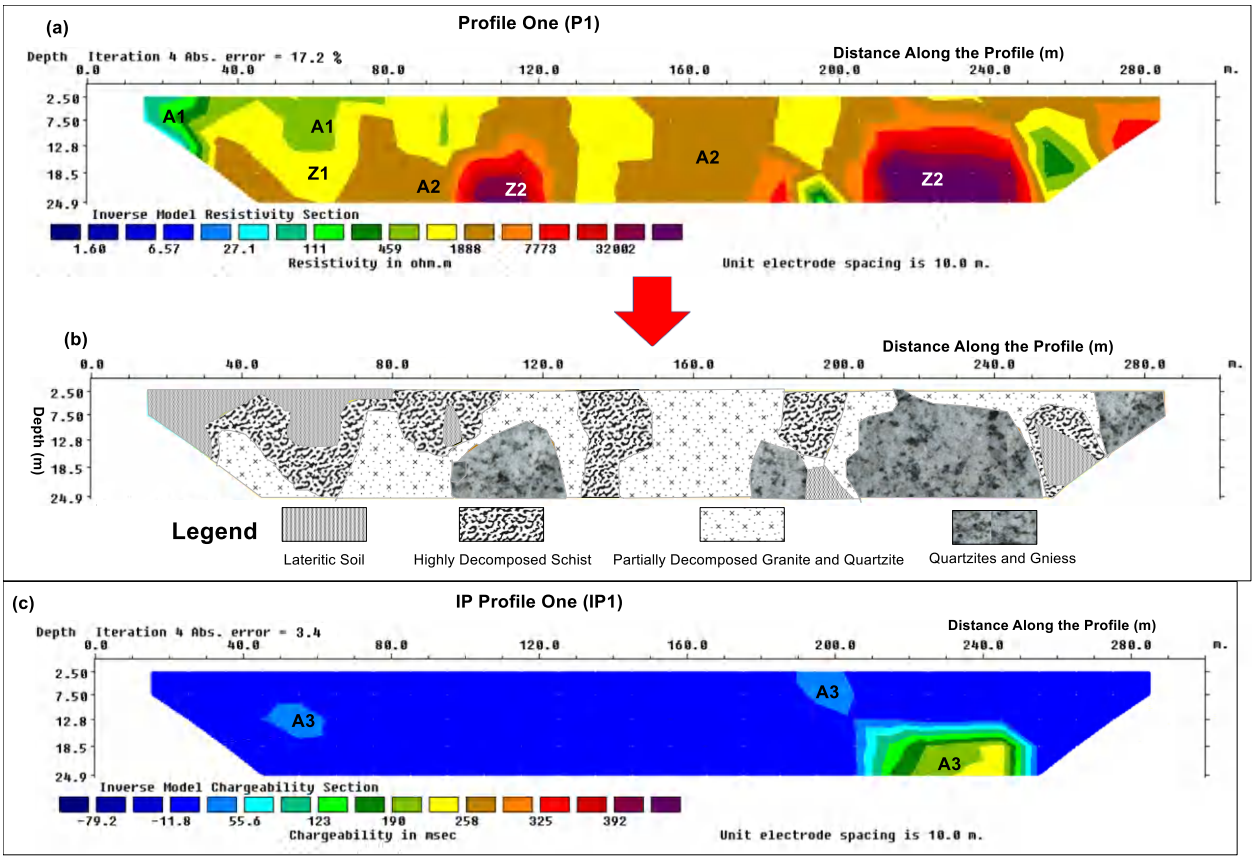

Figure 7: (a) Inverse model resistivity section (b) geologic section and (c) inverse model chargeability section for the dataset along profile three (P3)

Figure 7c shows the outcomes of the 2D inverse model chargeability sections along profile 1 (IP1). Zone **A3**, the area exhibiting metallic minerals, was clearly identified in the sections. These areas have the most notable chargeability values (≥ 20 msec). It covers x-positions of 45–60 m, 190–202 m, and 202-255 m, with corresponding depths and thicknesses of 7.5–18.5 m, 7.5 m, and 12.8–24.9 m. The accumulation of metallic minerals in host rocks is usually the cause of zone **A3**'s higher chargeability. These locations may be investigated as potential targets for the study of particular metallic minerals, especially gold mineralisation.

Geoelectric Sections for Profile 2

The result of 2D resistivity Profile 2, which has a lateral extent of 300 m, is displayed in Figure 8a. It is situated between latitudes 10°48'7.2"N and 10°48'0"N and longitudes 4°45'0"E and 4°45'7.2"E, with an orientation of NW-SE (refer to Figure 2). The differences in subsurface resistivity were divided into zones **A1**, **Z1**, **A2**, and **Z2**. The subsurface variations for these zones are summarised in Table 2 with respect to the area's borehole lithology as provided in Table 1 and the resistivity of common rocks.

The main areas of likely gold mineralisation were found to be zones **A1** and **A2**, which are low and high

resistivity values, respectively. The low resistivity zone (**A1**) may be the product of weathering in an oxidized rock, which is typically composed of granite or rhyolite, based on the geological setting of the research region. It might therefore be connected to specific minerals, especially gold. However, a high resistivity zone (**A2**) produced the dyke structures connected to partially decomposed granite and quartzite. These structures may play a key role in the identification of mineralisation, especially that of gold. Based on these findings, the geologic section that is shown in Figure 8b was created.

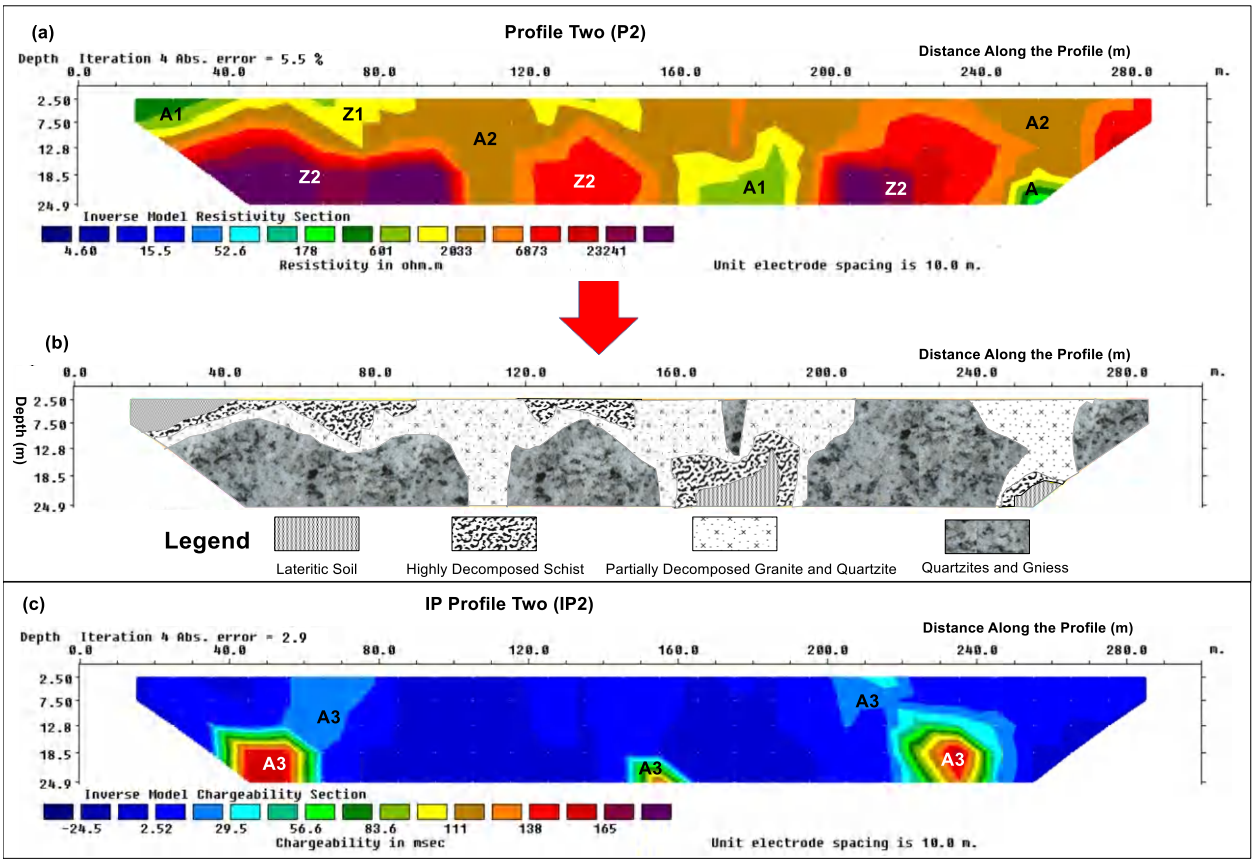

Figure 8: (a) Inverse model resistivity section, (b) geologic section and (c) inverse model chargeability section for the dataset along profile two (P2)

Figure 8 (c) presents the chargeability section results of the 2D inverse model for profile two (IP2). Zone **A3**, the region with potential for mineralisation, was amply highlighted in the sections of this profile. Because of the concentration of metallic minerals in the host rocks, these areas have a tendency to have higher chargeabilities. The lateral separations and depths that each zone occupies are shown in Table 2. Explicit metallic minerals, especially gold mineralisation, could be studied at these sites in the future.

Geoelectric Sections for Profile 3

Figure 9a shows the 2D resistivity model section along profile 5. It is located between latitudes 10°47'52.8"N and 10°47'45.96"N and longitudes 4°45'3.6"E and 4°45'10.8"E, that extend a lateral distance of 300 m (refer to Fig. 2). Zones **A1**, **A2**, **Z1**, and **Z2** were assigned to the subsurface resistivity signature based on the resistivity of the local geology and the rock formation. Table 2 provides the suggested subsurface lithology for features **A1**, **A2**, **Z1**, and **Z2**.

Zone **A1** relates to oxidized granite/quartzite and gneiss; based on geological contexts and the resistivity of common rocks, it can typically be associated to specific minerals, mostly gold (Table 1). For metallic minerals, Zone **A2** is another promising zone that produced the dyke structures attributed to partially decomposed granite and quartzite. These structures could play a key role in identifying mineralised zones, particularly those with gold mineralisation. The profile's findings led to the development of the geologic section which is shown in Figure 9b.

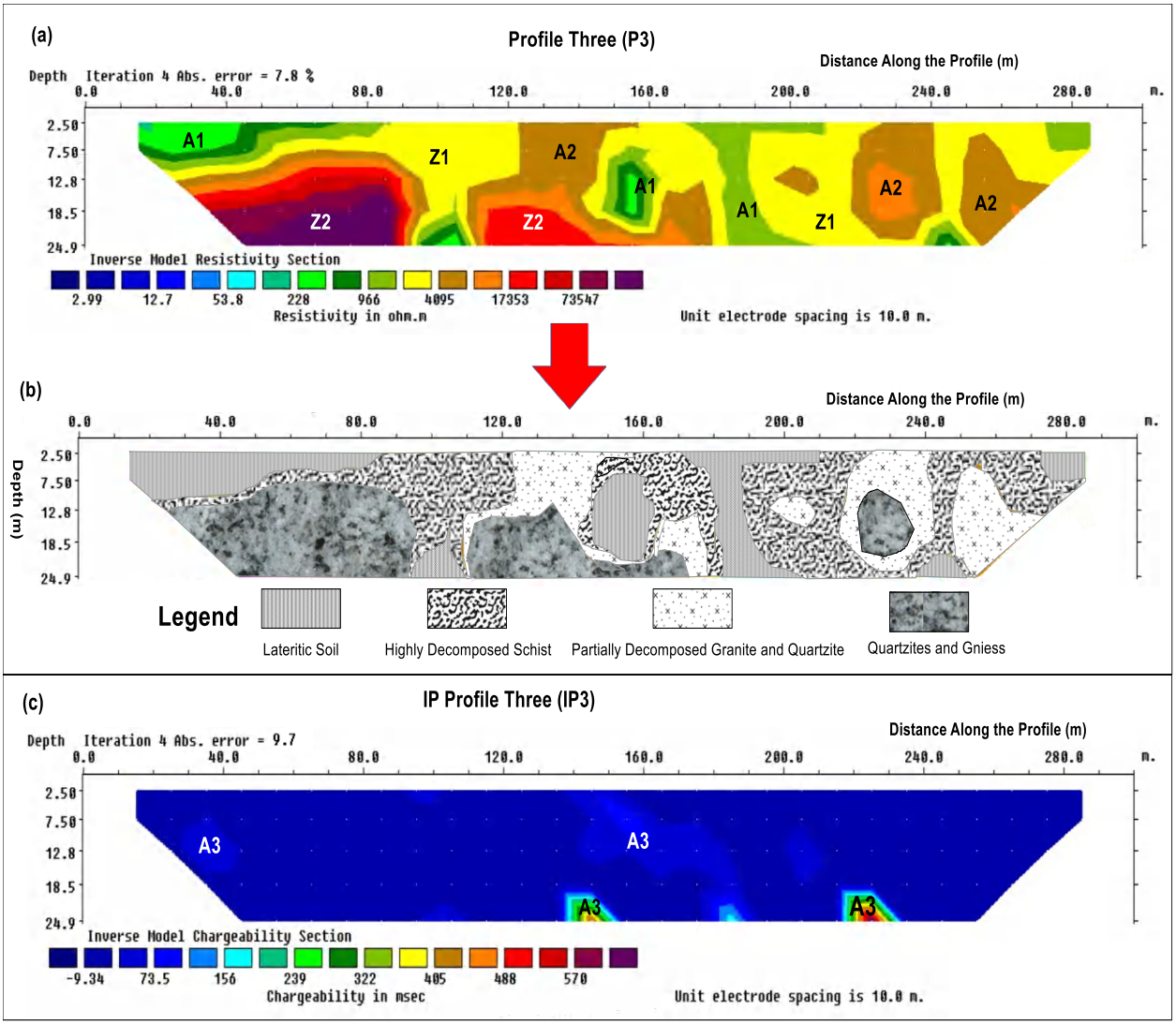

Figure 9: (a) Inverse model resistivity section, (b) geologic section and (c) inverse model chargeability section for the dataset along profile three (P3)

Chargeability sections along profile three (IP3) are depicted in Figure 9. The sections with the highest chargeability were indicated by Zone **A3**. The presence of metallic minerals in zones **A3** (70 msec and above) may result in higher chargeability. The length and depth of these zones are summarised in Table 2. These regions with the highest changeability might be thought of as likely potential for gold mineralisation exploration and exploitation.

Table 2: Summary of results obtained from the integrated methods

Profile	Resistivity Results				Induced polarisation Results				Probable gold mineralisation potential remarks
	Zone	Resistivity ranges (Ωm)	Lateral lengths (m)	Depth/ Thickness (m)	Zone	Chargeability ranges (msec)	Lateral lengths (m)	Depth/ Thickness (m)	
P1	A1	1.6 to 459	10-80, 190-200 and 250-265.	12.0, 18.5-24.9 and 7.5-18.5	A3	≥ 20	45-60, 190-202 and 202-255	7.5-18.5, 7.5 and 12.8-24.9	Yes
	Z1	460 to 1888	30-110, 130-149, 190-200 and 245-265	2.5-18.5, 24.9, 18.5 and 2.5-18.5	-	-	-	-	No
	A1	1889 to 7773	35-55, 70-92, 105-130, 145-180, 200-210 and 220-270	8-24.9, 3-24.9, 24.9, 24.8, 24.9 and 7.5	-	-	-	-	Yes
	Z2	7774 to 32002	100-125, 175-190, 200-250 and 265-290	7.5-24.9, 12-24.9, 2.5-24.9 and 18.5	-	-	-	-	No
P2	A1	4.6 to 601	5-40, 165-185, 245-260	7.5, 18.5-24.9 and 18.5-24.9	A3	20 and above	35-65, 55-80, 145-160, 200-220 and 221-250	12.8-24.9, 12.8, 18.5, 7.5 and 7.5-24.9	Yes
	Z1	602 to 2033	40-90, 120-150, and 155-190	12, 7.5 and 18.5-24.9	-	-	-	-	No
	A2	2034 to 6873	10-90, 95-120, 140-170, 180-205, 240-270	2.5-12.8, 24.9, 12.8, 12.8 and 18.5	-	-	-	-	Yes
	Z2	6874 to 23241	10-105, 115-155, 170-180, 200-245, and 270-290	7.5-24.9, 7.5-24.9, 12.8, 24.9 and 18.5	-	-	-	-	No
P3	A1	2.99 to 966	5-80, 90-105, 135-160, 170-190, 235-50 and 270-290	7.5, 18.5-24.9, 7.5-18.5, 24.9, 18.5-24.9 and 7.5	A3	70 and above	30-45, 135-150, 140-170 and 210-240	7.5-18.5, 18.5-24.9, 2.5-18.5 and 18.5	Yes
	Z1	967 to 4095	10-90, 91-120, 145-180, 190-220 and 240-270	3-7.5, 18.5, 12.8, 24.9, and 18.5	-	-	-	-	No
	A2	4096 to 17353	120-150, 160-175, 195-210, 220-240 and 250-270	12.8, 18.5-24.9, 12.8-18.5, 19 and 7.5-24.9	-	-	-	-	Yes
	Z2	17354 to 73547	10-90, 110-170 and 220-235	7.5-24.9, 12.8-24.9 and 12.8-18.5	-	-	-	-	No

Possible Potential Gold Mineralised Zones of the Area

Zones **A1**, **A2**, and **A3** are the proposed mineralization potential zones along geoelectric profiles 1, 2, and 3 (P1, P2, and P3 as well as IP1, IP2, and IP3). As seen in Figures 7-9, these regions are distinguished by signatures of high chargeability and low/high resistivity. The integrated key zones of potential gold mineralisation are shown in Figure 10. These zones may be considered as prospective locations for metallic mineral exploration, specifically in relation to gold mineralisation.

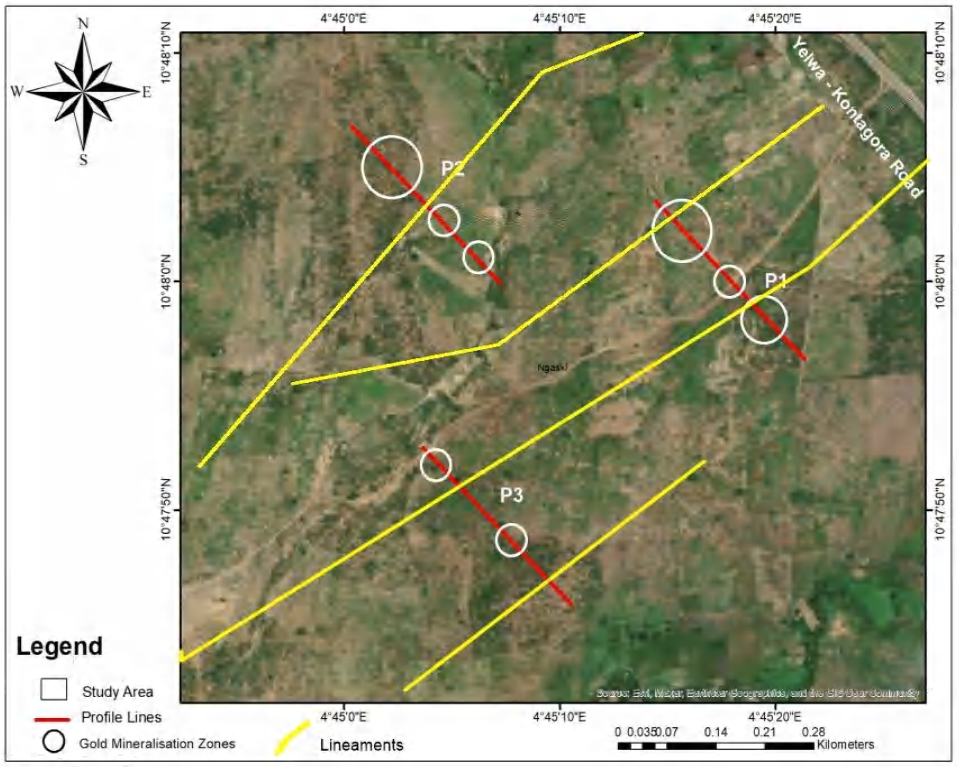

Figure 10: Major zones of gold mineralisation potentials map

CONCLUSION

This study employed integrated geophysical methods with which generated an updated structural features of the regions as well as database with precise locations, lateral lengths, thicknesses, and depths for prospective gold mineralisation zones. This database has the potential to enhance the regions of gold exploration activities. Major structural features identified in previous magnetic studies conducted in the region by Augie et al. (2021) and Augie et al. (2022a&b) were also confirmed by the study. The current study employed an aeromagnetic approach to identify potential gold mineralisation areas within the major structure, or lineament. The results obtained from this approach are consistent with those of prior aeromagnetic studies conducted in the same area. The locations found for structural feautures are in the northwest of Magama and the eastern portions of Yelwa (Yauri), Ngaski, Shanga, and Agwara. The eastern portions of Ngaski/Yauri have undergone further investigation using 2D ERT and IP detailed geophysical methods, resulting in one of the main lineament zones identified from aeromangnetic data. Zones **A1**, **A2**, and **A3** are the main areas with potential for gold mineralisation that were identified by the geoelectric method along profiles 1, 2, and 3. These areas may be potential target zones for the exploration of metallic minerals, particularly gold mineralisation, as they exhibit low/high resistivity and chargeability signatures. These regions These regions are located in Kebbi State around Jinsani areas to the southwest of Mararraba's northern region.

DATA AVAILABILITY

The acquired and generated datasets in the current study are not available to the general public due to the following reasons: (a) Aeromagnetic data are under the custody of the Nigeria Geological Survey Agency (NGSA) and can only be released upon request and payment via their website (https://ngsa.gov.ng), and (b) resistivity and induced polarisation data generated in this study area are available from the corresponding author on reasonable request.

ACKNOWLEDGEMENTS

The authors would like to express their profound appreciation to the Tertiary Education Trust Fund (TETFund) for funding this research as well as the management of the Nigeria Geological Survey Agency (NGSA) for the release of the airborne magnetic dataset. Our thanks are also extended to the district heads of Mararraba of Yelwa Yauri area of Kebbi state for approval of the site to collect geophysical data. Our appreciation also goes to the Department of Physics, Bayero University Kano and the Department of Geophysics, Federal University of Technology Minna for providing the instruments as well as Geosoft Inc. for the use of Oasis Montaj and Res2dinv Softwares.

REFERENCES

Adetona, A.A., Kwaghhua, F.I. & Aliyu, S.B. (2022). Interpreting the magnetic signatures and radiometric indicators within Kogi State, Nigeria for economic resources. Geosystems and Geoenvironment, 2, 100157, https://doi.org/10.1016/j.geogeo.2022.100157

Aisabokhae, J.E. (2021). Geophysical mapping and mineralisation characterisation of the mesothermal auriferous basement complex in southern Kebbi, NW Nigeria. NRIAG Journal of Astronomy and Geophysics, 10(1), 443-465, https://doi.org/10.1080/20909977.2021.2005333

Aliyu, S.B, Adetona, A.A., Rafiu, A.A., Ejepu, J. & Adewumi, T. (2021). Delineating and interpreting the gold veins within Bida and Zungeru area, Niger state Nigeria, Using aeromagnetic and radiometric data. Pakistan Journal of Geology (PJG), 5(2), 41-50.

Augie, A.I., Salako, K.A., Rafiu, A.A. & Jimoh, M.O. (2021). Estimation of depth to structures associated with gold mineralisation potential over southern part of Kebbi State using aeromagnetic data. [in:] 3rd School of Physical Sciences Biennial International Conference Futminna 2021, Federal University of Technology Minna, 290–297.

Augie, A.I., Salako, K.A., Rafiu, A.A & Jimoh, M.O. (2022a). Geophysical assessment for gold mineralisation potential over the southern part of Kebbi State using aeromagnetic data. Geology, Geophysics & Environment, 48 (2), 177–193. https://doi.org/10.7494/geol.2022.48.2.177.

Augie, A.I., Salako, K.A., Rafiu, A.A. & Jimoh, M.O. (2022b). Geophysical magnetic data analyses of the geological structures with mineralisation potentials over the southern part of Kebbi, NW Nigeria. Mining Science, 29, 179–203, https://doi.org/10.37190/msc222911

Bonde, D.S., Lawali, S. & Salako, K.A. (2019). Structural mapping of solid mineral potential zones over southern part of Kebbi state, northwestern Nigeria. Journal of Scientific and Engineering Research 6(7), 229-240.

Core, D., Buckingham, A. & Belfield, S. (2009). Detailed structural analysis of magnetic data-done quickly and objectively. SGEG New, 1(2), 15–21.

Holden, E.J., Dentith, M. & Kavesi, P. (2008). Towards the automatic analysis of regional aeromagnetic data to identify regions prospective for gold deposits. Computer Geoscience, 34, 1505–1513, https://doi.org/10.1016/j.cageo. 2007.08.007

Lawal, M.M., Salako, K.A., Abbas, M., Adewumi, T., Augie, A.I. & Khita, M. (2021). Geophysical investigation of possible gold mineralization potential zones using a combined airborne magnetic data of lower Sokoto basin and its environs Northwestern Nigeria. International Journal of Progressive Sciences and Technologies (IJPSAT), 30(1), 01-16.

Lawali, S., Salako, K.A. & Bonde, D.S. (2020). Delineation of mineral potential zones over lower part of Sokoto Basin, northwestern Nigeria using aeromagnetic data. Academic Research International, 11(2), 19–29.

Loke, H.M. (1999). Electrical imaging surveys for environment and engineering studies (practical guide to 2D and 3D survey). Earth Science, 44(1), 131–152.

Loke, M. (2000). Rapid least-square inversion of apparent resistivity pseudosections. Earth Science, 64(3), 31–52.

Loke, M.H. & Barker, R.D. (1996). Rapid least-squares inversion of apparent resistivity pseudosections using a Quasi-Newton method. Geophysical Prospecting, 44, 131-152.

NGSA (2006). Nigerian Geological Survey Agency, Nigeria.

Olugbenga, T. T. & Augie, A. I. (2020). Estimation of crustal thickness within the sokoto basin north-western Nigeria using bouguer gravity anomaly data, WASET, International Journal of Geological and Environmental Engineering, 14(9), 247– 252

Osazuwa, I.B. & Chii, E.C. (2010). Two-dimensional electrical resistivity survey around the periphery of an artificial lake in the precambrian basement complex of

northern Nigeria. International Journal of Physical Science 5(3), 238–245.

Ramadan, T.M. & AbdelFattah, M.F. (2010). Characterization of gold mineralization in Garin Hawal area, Kebbi State, NW Nigeria, using remote sensing. Egyptian Journal of Remote Sensing and Space Science 13(2), 153–163. https://doi.org/10.1016/j.ejrs.2009.08.001

Sani, A.A., Augie, A.I. & Aku, M.O. (2019). Analysis of gold mineral potentials in Anka schist belt north western Nigeria using aeromagnetic data interpretation. Journal of African Earth Sciences, 52, 291-298.

SARDA (1988). Sokoto agricultural and rural development authority: Sokoto Fadama.

Wahyu, S., Trimadona, P. & Pratomo, M. (2016). 2D Resistivity and induced polarisation measurement for manganese ore exploration. Journal of Physics: Conference Series, 739, https://doi.org10.1088/1742-6596/739/1/012138